PCCP

Physical Chemistry Chemical Physics

rsc.li/pccp

ROYAL SOCIETY
OF CHEMISTRY

PAPER
Sergiu M. Gorun, Derck Schlettwein *et al.*
The influence of intermolecular coupling on electron and ion
transport in differently substituted phthalocyanine thin films
as electrochromic materials: a chemistry application of the
Goldilocks principle

The influence of intermolecular coupling on electron and ion transport in differently substituted phthalocyanine thin films as electrochromic materials: a chemistry application of the Goldilocks principle†

Thi Hai Quyen Nguyen,[a] Marius Pelmuş, [ID][b] Christopher Colomier, [ID][b] Sergiu M. Gorun [ID] *[b] and Derck Schlettwein [ID] *[a]

The transport of both electrons and ions in organic mixed ionic and electronic conductors such as phthalocyanines, is essential to allow redox reactions of entire films and, hence, to impart electrochromism. Thin films of a new type, tetrakis-perfluoroisopropyl-perfluoro phthalocyanine, **F₄₀PcCu** of different thicknesses were obtained *via* vapor deposition. The extent of the intermolecular coupling within the **F₄₀PcCu** films established by van der Waals interactions was investigated by *in situ* optical spectroscopy during film growth. The transfer of electrons and diffusion of counter cations in these films, as well as their electrochromic performance were characterized by electrochemical and spectroelectrochemical measurements with an aqueous solution of KCl as electrolyte. A moderate degree of intermolecular interaction of the **F₄₀PcCu** molecules in the solid state was observed, compared to non-fluoroalkylated perfluoro phthalocyanine, **F₁₆PcCu** and octakis-perfluoroisopropyl-perfluorophthalocyanine, **F₆₄PcCu**, which exhibit stronger and weaker coupling, respectively. The replacement of F by perfluoroisopropyl is, thereby, established as a valuable approach to tune this coupling of chromophores and, hence, the transport coefficients of electrons and ions in the solid films. Reversible changes of the films upon reduction and intercalation of K⁺ counter ions and re-oxidation and expulsion of the counter ions were confirmed by simultaneously measured optical absorption spectra. Thin films of **F₄₀PcCu** showed a well-balanced, equally fast transport of electrons and ions. The films provided a fast and reversible switching process over at least 200 cycles indicating the stability of these materials.

1 Introduction

Molecular thin films play an increasingly important role in electronic and optoelectronic devices as dielectric, conducting or semiconducting materials.[1] One specific example is their use as electrochromic layers, *i.e.* layers which reversibly change their color and/or light transmission upon their reduction or oxidation. Such layers are of potential use in display applications or as smart windows or smart mirrors.[2,3] When compared to classic electrochromic materials like WO₃, organic materials

offer faster switching due to their higher extinction coefficients which allow the use of thinner films.[4,5] In order to establish such higher switching rates, the diffusion of ions and the mobility of electrons in the films have to be optimized since both are needed at a given molecular site in the films in order for the redox reaction to occur. As a consequence, organic mixed ionic and electronic conductors (OMIEC) are needed for this purpose, a group of materials recently established in the literature.[6] For a number of such materials, namely polymer electronic (or hole-) conductors, water is needed in the films in order to provide channels of ionic conduction – polymers are chosen that are easily swollen with water.[7,8] Electrochromic reactions, however, have also been established for pure molecular semiconductors, namely phthalocyanines (Pc).[9]

In early studies, unsubstituted Pc (*e.g.*, **H₁₆PcCu**, Fig. 1a) showed partially reversible electrochromic oxidation.[10] Substitution of aromatic hydrogen atoms by electron-withdrawing groups facilitate an electrochromic reduction characterized by a highly increased reversibility.[11] Unsubstituted Pc, as well as

[a] *Institute of Applied Physics and Laboratory of Materials Research, Justus-Liebig-University Gießen, Heinrich-Buff-Ring 16, 35392 Gießen, Germany. E-mail: schlettwein@uni-giessen.de*

[b] *Department of Chemistry and Biochemistry and Center for Functional Materials, Seton Hall University, 400 South Orange Ave, South Orange, NJ 07079, USA. E-mail: sergiu.gorun@shu.edu*

This journal is © the Owner Societies 2020

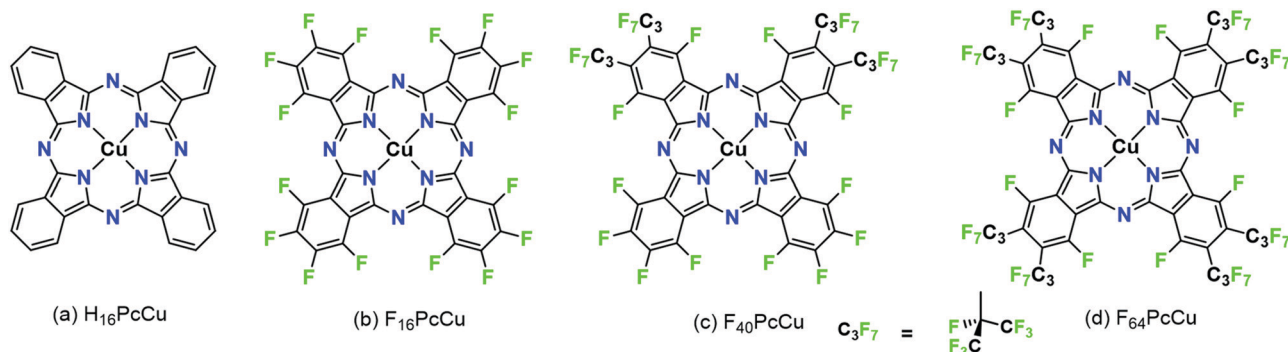*Phys. Chem. Chem. Phys.*, 2020, **22**, 7699–7709 | 7699

Fig. 1 Structural formulae of copper phthalocyanines with different degree of fluorination.

suitably substituted Pc can be sublimed to form thin films by physical vapor deposition (PVD) on a variety of substrates. In the solid state, such Pc molecules typically form molecular crystals bound by van der Waals (vdW) interactions.[12] The weak intermolecular interactions result in polycrystallinity for a given molecule, *e.g.* α- and β-phases of unsubstituted Pc[13] or a variety of structures in thin films of, *e.g.* perfluorinated $F_{16}Pc$.[14] Different intermolecular orientations in these different crystalline phases leads to significant differences in the electronic coupling of the central aromatic chromophore systems and, hence, significant differences in their optical absorption spectra.[15] The strength of intermolecular vdW interactions in Pc molecules in solids can further be rationally tuned by a judicious choice of the substituents of the aromatic macrocycles, detected in the absorption spectra of thin films.[16,17] In a direct comparison of vapor-deposited thin films of a perfluorinated copper phthalocyanine, $F_{16}PcCu$ (Fig. 1b), with those of a copper phthalocyanine in which the eight non-peripheral 8 H-atoms of the parent $H_{16}PcCu$ had been substituted by F-atoms and the other, peripheral 8 H-atoms were substituted by perfluoroisopropyl groups, $F_{64}PcCu$ (Fig. 1d) it could be shown that the films of $F_{16}PcCu$ exhibit strong electronic coupling, also leading to their crystallinity, whereas those of sterically hindered $F_{64}PcCu$ showed very weak coupling, in line with amorphous growth.[18]

Films of both $F_{64}PcCu$ and $F_{16}PcCu$ exhibited electrochromic switching upon their reduction and subsequent re-oxidation. However, in accordance with the strength of vdW interactions and, hence, electronic coupling of the aromatic macrocycle, the rate of switching in films of $F_{16}PcCu$ was limited by ion diffusion (high electron mobility), as opposed to the switching rate in films of $F_{64}PcCu$ that was limited by electron conduction (fast ion diffusion). These limiting cases, linked to the limiting structural features imparted by the lack or presence of bulky fluoroalkyl substituents, respectively, suggested that the optimization of the substitution pattern and, thus, of the vdW interactions of Pc molecules in the solid state could result in a molecule exhibiting sufficiently strong interactions favoring a high electronic coupling and thus electron mobility, but also still sufficiently weak to facilitate fast diffusion of charge-compensating ions in films.

Following this strategy (the "Goldilocks principle"), $F_{40}PcCu$ was synthesized and characterized in the present work, Fig. 1c. In $F_{40}PcCu$ 12 H-atoms of $H_{16}PcCu$ are formally substituted by F but only 4 by perfluoroisopropyl groups. $F_{40}PcCu$ exhibits an intermediate degree of steric hindrance, electronic deficiency and likely an intermediate strength of vdW interactions, therefore, a likely optimized balance between electron mobility and ion diffusion. Fast, reversible electrochromic switching is indeed realized in this optimized OMIEC and the consequences for technical application of potential devices are discussed below.

2 Experimental

2.1 Synthesis

Tetrafluorophthalonitrile, **1**, 0.016 g (0.08 mmol), perfluoro-(4,5-diisopropyl)phthalonitrile, **2**, 0.1 g (0.2 mmol), and copper(II) acetate monohydrate, 0.015 g (0.08 mmol), were mixed with a few drops of nitrobenzene in a glass vial, sealed with a Teflon cap and heated in a microwave reactor at 185 °C for 12 minutes. The crude products were separated *via* gravity column chromatography using silica gel 60 (63–200 µm) and a 0–15% gradient of ethyl acetate in hexanes, followed by an isocratic 30% ethyl acetate/hexanes blend to yield a mixture of $F_{64}PcCu$, $F_{52}PcCu$ and $F_{40}PcCu$. The phthalocyanines were separated using flash chromatography in 0–50% CH_2Cl_2/hexanes. $F_{40}PcCu$ was isolated as a deep-blue solid in 17% yield. UV-Vis (TFT): λ_{max} (log ε) 686 (5.33), 616 (4.64), 360 (4.85) nm (L mol^{-1} cm^{-1}); UV-Vis (ethanol): λ_{max} (log ε) 676 (4.95), 640 (4.74), 612 (4.49), 372 (4.62), 316 (4.52) nm (L mol^{-1} cm^{-1}); HRMS (ESI, negative mode, Fig. S1 in ESI†): calculated for $C_{44}F_{40}N_8Cu + Cl^-$ [M + Cl]$^-$ 1497.8586, found 1497.8611 (δ = 16.7 ppm), FT-IR (KBr disk) ν, cm^{-1} (intensity), Fig. S2 (ESI†): 2918.53 (w), 2850.76 (w); 1527.97 (w), 1491.21 (w) C=C aromatic; 1251.43 (s), 1171.29 (m), 1104.90 (w), C–F aliphatic and aromatic; 964.30 (w), 729.74 (w), 752.33 (w), 470.64 (w).

2.2 Chemicals and molecular characterization

All solvents (ACS grade or better) and reagents were purchased from commercial sources and used as received, unless stated otherwise. Copper acetate monohydrate and the fluorinated tetrafluorophthalonitrile, **1**, (Fig. 2) were purchased from TCI Co., Ltd. Perfluoro-(4,5-diisopropyl)phthalonitrile, **2**, was prepared as described in the literature.[19] $F_{16}PcCu$ was purchased from TCI in sublimed grade, $F_{64}PcCu$ was prepared as described in ref. 16.
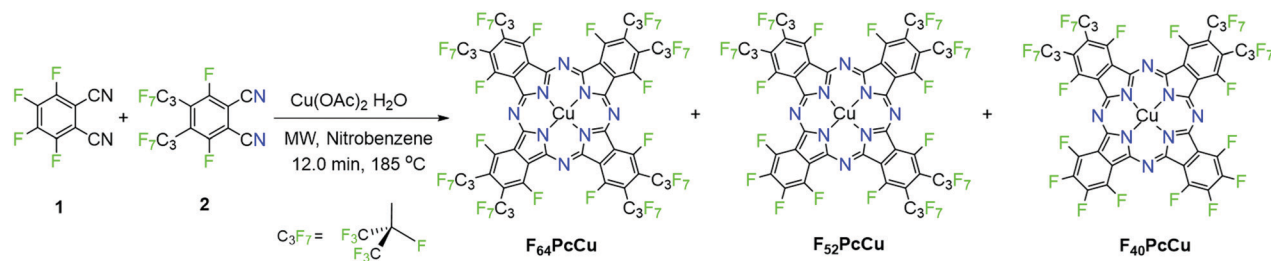
Fig. 2   Reaction scheme for the synthesis of perfluorinated copper phthalocyanines.

The microwave-assisted syntheses were performed using a CEM Discover system (CEM Corporation). Flash chromatography was carried out using a CombiFlash Rf+, (Teledyne ISCO). UV-Vis spectra were recorded on a Cary 500 Scan UV-Vis-NIR spectrophotometer. FT-IR spectra were recorded on a Nicolet 4700 FT-IR spectrophotometer using KBr pellets. High-resolution mass spectrometry (HRMS) data were obtained at Rutgers University (Newark, NJ) by direct injection of ethanolic solutions in an Apex-ultra 70 hybrid FT-MS. For the electrochemical investigations by CV (cyclic voltammetry) at a scan rate of 0.1 V s^{-1} and SWV (square wave voltammetry at a pulse amplitude of 50 mV, a frequency of 10 Hz and a potential step of 5 mV), solutions of the molecules in 0.1 M tetrabutylammonium tetrafluoroborate (TBATFB, Fluka, 99%, electrochemical grade) in trifluorotoluene (TFT, Sigma-Aldrich, ≥99%) were used. The measurements were carried out employing an IviumStat potentiostat/galvanostat, equipped with Pt wires as working electrode and counter electrode, respectively, and a leak-free Ag/AgCl reference electrode (LF-2, Innovative Instruments, Inc.) for which the potential was calibrated against ferrocene/ferrocenium (Sigma-Aldrich, 98%) at 0.4 V vs. Ag/AgCl[20] in dimethylformamide (Sigma-Aldrich, 99.8%). All experiments were performed at room temperature in a glovebox under dry nitrogen.

2.3   Preparation of thin films

Glass substrates coated with FTO (Kaivo, <15 Ohm sq^{-1}) were cut into 10 mm × 25 mm pieces. The FTO-coated glass pieces were cleaned for 15 min in RBS solution (Roth), acetone (Roth, ≥99.5%) and isopropanol (Roth, ≥99.8%), respectively, using an ultrasonic bath at room temperature. The cleaned substrates were dried with N$_2$ gas. A piece of adhesive tape from TESA was attached to the shorter edge of the substrate in order to keep an area of the substrate uncovered for later electrical contacting.

Thin films with different thicknesses of **F$_{40}$PcCu** were prepared on FTO-coated glass by physical vapor deposition in a vacuum chamber with a quartz crystal microbalance which was calibrated as reported in ref. 16 for monitoring the deposited mass and calculating an average film thickness based on an estimated density (2.2 g cm^{-3}) as an average value from the known values of **F$_{16}$PcCu** and **F$_{64}$PcCu**.[13,16] The vapor deposition was carried out at a pressure of <10^{-6} mbar and an evaporation rate of about 0.5–1 nm min^{-1} by resistively heating the powder of **F$_{40}$PcCu** in a BN crucible (Kurt J. Lesker Ltd). In order to analyze the thickness-dependent film growth of **F$_{40}$PcCu**, an optical fiber was attached to the vacuum chamber

and a pre-cleaned quartz glass (TED PELLA, INC.) was mounted into the chamber as a substrate. A lower deposition rate of 0.2 nm min^{-1} was chosen to allow measurements of the optical absorption spectra by a tec 5 diode array spectrometer during deposition at a pressure of <10^{-5} mbar. The sample was rotated between two positions to alternately vapor-deposit the film and measure the spectra as reported earlier.[16]

2.4   Characterization of thin films

The film coverage on the substrate and cross-sections of the films were analyzed by scanning electron microscopy (SEM) in a Zeiss MERLIN at an emission current of 100 pA and an acceleration voltage of 5 kV. The film morphology was investigated by atomic force microscopy (AFM) in air using a Smart SPM 1000 (AIST-NT) with NanoWorld Pointprobe SEIHR Non-Contact/Soft Tapping probes (tip radius < 12 nm) in an oscillating mode. Images were processed by the Gwyddion 2.55 program using the plane subtraction method and adjusting the individual lines by the median of differences. The crystallinity of the thin films was analyzed by grazing incidence X-ray diffractometry using a PAN-analytical X'Pert Pro MRD instrument with Cu-K$_\alpha$-radiation. The spectroelectrochemical analysis of the films was performed in a 1 M aqueous KCl (Aldrich, ≥99.5%) solution with a three-electrode setup. To remove the dissolved oxygen from the solution, N$_2$ gas was flushed through the solution before the measurements. During the measurements, N$_2$ gas was passed above the surface of the solution only, to avoid fluctuation of the solution. To contact the fluorinated phthalocyanine films for the spectroelectrochemical characterization, a Cu wire was attached with conductive Ag paste (Ferro GmbH) on the uncovered substrate area. Afterwards, the metal wire and the substrate area were sealed with Araldite Rapid epoxy resin. The prepared sample was mounted as working electrode in a glass cell (Starna) with a platinum wire counter electrode (Goodfellow, 99.995%) and a Ag/AgCl reference electrode (REF201 Red Rod, Radiometer analytical). Cyclic voltammetry between 0.6 V and −1.1 V at different scan rates and chronoamperometry between the bias potentials of 0.6 V and −1.0 V at a time delay of 3 s were carried out employing an IviumStat potentiostat/galvanostat. Optical spectra were simultaneously measured in situ by placing the working electrode into the beam of the tec5 diode array spectrometer. The charge measured during long-term switching experiments is underestimated by a factor of about 3.8 which is caused by a rather low sampling frequency (5 Hz compared to 1 kHz) needed to ensure reliable data acquisition by the spectrometer.

3 Results and discussion

3.1 Synthesis and properties of F$_{40}$PcCu

The synthesis method, Fig. 2, uses two different precursors with different propensities to form phthalocyanines. The ratio of precursors **1** vs. **2** is 2:2 in **F$_{40}$PcCu**, but a ratio of 0.08/0.2 = 0.8:2 was used in order to minimize the formation of the 4:0 complex **F$_{16}$PcCu**. The complexes 1:3, **F$_{52}$PcCu** and 0:4, **F$_{64}$PcCu**, Fig. 2, also form, but the reported **1** vs. **2** ratio seems to give **F$_{40}$PcCu** in modest but maximum isolated yield. Further optimizations of either the reaction conditions or the purification method were not pursued. The structure of **F$_{40}$PcCu**, Fig. 2, depicts the complex in its "*cis*" form, with the two coordinating, C$_3$F$_7$-substituted isoindole rings, labeled 'isoR' adjacent, *i.e.* the N$_{isoR}$–Cu–N$_{isoR}$ angle is 90°. Alternatively the rings can be "*trans*", the N$_{isoR}$–Cu–N$_{isoR}$ angle being 180°. The assignment, in the absence of a single-crystal X-ray structure is based on the structure of the analogous F$_{40}$PcCo complex, for which an X-ray crystal structure has been reported.[21]

The spectral position of the Q-band of **F$_{40}$PcCu** in solution (Fig. 3) corresponds to that reported for F$_{40}$PcZn or F$_{40}$PcCo,[22] for which the "*cis*" structure of the substituents was proven, in good agreement with literature reports on Q-band differences for complexes in either "*cis*" or "*trans*" structure.[23,24] Our assignment of a "*cis*" structure for **F$_{40}$PcCu**, therefore, is fully consistent with the literature.

F$_{40}$PcCu exhibits solvent dependent UV-Vis spectra, Fig. 3. The main Q-band in TFT, 686 nm, appears at least twice as intense as the one in ethanol, 676 nm. The Beer–Lambert plots of concentration dependent spectra, Fig. S3 and S4 (ESI†), are linear, but the variation of absorbance of the Q-band with concentration is approximately double in TFT vs. ethanol. Taken together, the data suggest that a higher degree of aggregation exists in ethanol, consistent with ethanol axial coordination in **F$_{64}$PcCu**.[25]

Cyclic voltammetry (CV) and square wave voltammetry (SWV) were performed for solutions of **F$_{40}$PcCu** in direct comparison to solutions of **F$_{16}$PcCu** and **F$_{64}$PcCu** in order to discuss the
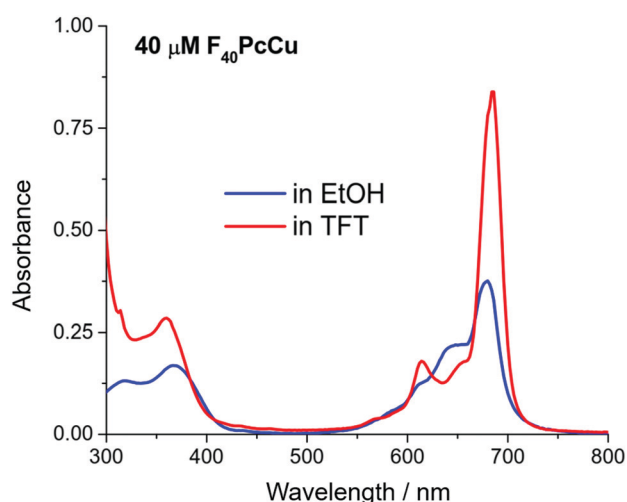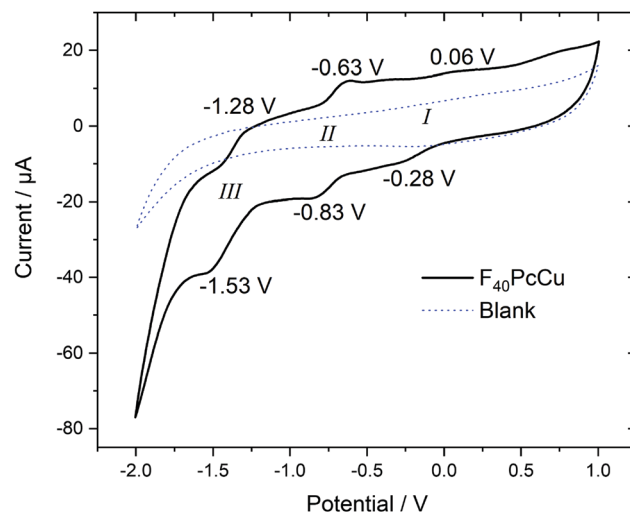

Fig. 4 Cyclic voltammetry at 0.1 V s^{-1} of **F$_{40}$PcCu** dissolved in 0.1 M TBATFB in TFT compared to a blank scan of the electrolyte in the absence of **F$_{40}$PcCu**.

influence of substituents on the redox potential of reduction reactions under otherwise identical conditions. The CV results for the new complex **F$_{40}$PcCu** are shown in Fig. 4 and the main findings are summarized together with the SWV results for all complexes in Table 1. Values measured for **F$_{16}$PcCu** reveal a potential for the first reduction (*I*) of −0.2 V and of the second reduction (*II*) of −0.9 V. The potential of *I* is found slightly less negative than the reported −0.6 V measured for the Zn-complex of F$_{16}$Pc in dimethylformamide, whereas that of *II* is found in accordance with the reported value (−0.9 V).[26] The values for **F$_{64}$PcCu** are found similar to those reported under comparable conditions[17] of *I* = −0.06 V, *II* = −0.56 V and *III* = −1.17 V.

The redox potentials indicate that **F$_{64}$PcCu** is easiest to reduce, followed by **F$_{40}$PcCu**, and **F$_{16}$PcCu**. This is consistent with the stronger electron-withdrawing effect of the C$_3$F$_7$ substituents vs. F atoms. The broad characteristics in the region of *I* speak in favor of a parallel reduction of differently aggregated species of **F$_{40}$PcCu** at this concentration needed to obtain reasonably high signals above background. Some small additional waves are detected which can be caused by solvent interaction with monomeric species, as also observed earlier for **F$_{64}$PcCu**.[17]

3.2 Film growth of F$_{40}$PcCu

Uniformly blue thin films, obtained after vapor deposition of **F$_{40}$PcCu** showed a compact film morphology consisting of

Fig. 3 UV-Vis spectra of **F$_{40}$PcCu** in ethanol (EtOH) and trifluorotoluene (TFT).

Table 1 Redox potentials (*E* in V vs. Ag/AgCl) of the redox waves of **F$_{16}$PcCu**, **F$_{40}$PcCu** and **F$_{64}$PcCu** in solution obtained from CV (0.1 V s^{-1}) and SWV experiments

Wave	Method					
	CV			SWV		
E/V	*I*	*II*	*III*	*I*	*II*	*III*
F$_{16}$PcCu	−0.21	—	—	−0.19	−0.88	−1.64
F$_{40}$PcCu	−0.11	−0.73	−1.40	—	−0.71	−1.40
F$_{64}$PcCu	0.05	−0.53	—	0.02	−0.49	−1.40

7702 | *Phys. Chem. Chem. Phys.*, 2020, **22**, 7699–7709
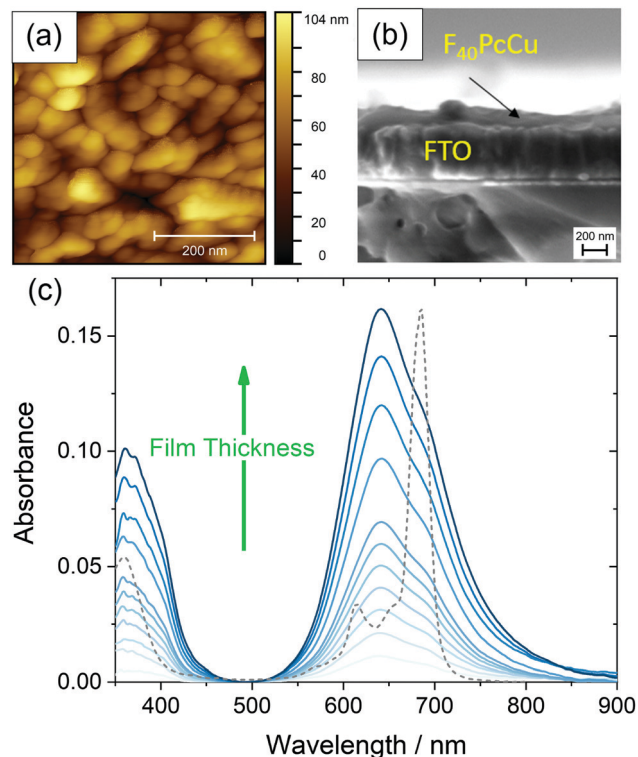
This journal is © the Owner Societies 2020

Fig. 5 Morphology of a 35 nm thin film of $F_{40}PcCu$ on FTO measured by AFM (a), cross-section of a 35 nm thin film $F_{40}PCu$ on FTO observed by SEM (b) and optical absorbance spectra acquired during film preparation of $F_{40}PcCu$ with a film thickness d of 0–35 nm on quartz glass at room temperature, the optical spectrum of $F_{40}PcCu$ in TFT (see Fig. 3) is shown as a dashed line (c).

individually contacted grains around 60–100 nm lateral diameter, in a similar range compared to $F_{64}PcCu$ (200 nm)[18] or $F_{16}PcCu$ (50 nm)[18] as revealed by AFM (Fig. 5a). The covering film of $F_{40}PcCu$ on FTO is also observed in the SEM cross-section (Fig. 5b). The extent of intermolecular electronic coupling of $F_{40}PcCu$ in thin films was monitored by *in situ* measurements of the optical absorption spectra during film growth (Fig. 5c). For all spectra, the Soret band below 400 nm[27] and the Q-band around 500–800 nm[27,28] characteristic for phthalocyanines were found. When compared to solution spectra (Fig. 3 and dashed line in Fig. 5c), which is dominated by the characteristic vibronic fine structure, the films showed significant broadening and a splitting of the Q-band revealing more intense interaction of the molecules in the solid state compared to solutions.[28,29] The splitting leads to a maximum at shorter wavelength which indicates dominance of face-to-face coupling of the molecules (H-aggregation) in solid state.[28,29] The presence of an absorption maximum around 640 nm and a shoulder at about 690 nm implies a structure similar to the α-structure of unsubstituted phthalocyanines with a herringbone orientation of the molecules.[15] Ultrathin films of $F_{16}PcCu$ in the range of a few monolayers[30,31] showed similar features typical for the β-bilayer structure with a parallel stacking of the molecules. Since the $F_{40}PcCu$ molecule contains bulky perfluoroisopropyl substituents, a molecular orientation appears likely where the chromophores are

not fully stacked as in the β-bilayer structure, but are oriented slightly inclined thereby approaching an orientation similar to the classic α-structure. The X-ray diffraction pattern (Fig. S5, ESI†) of a thin film of $F_{40}PcCu$ on FTO exhibits two reflections at around 6° and 19°. Their broad shape indicates the presence of films with a rather well-defined intermolecular orientation, but with still widely amorphous character. The positions of the peaks correspond to the (200) and (600) reflections of a herringbone orientation of the molecules parallel to the substrate as reported earlier for $F_{16}PcCu$ and PcCu thin films.[32,33] These results, therefore, confirm the presence of an α-structure as also derived from the optical analysis. The films grew at constant band positions and constant band splitting from the monolayer regime up to the film thicknesses studied in this work (Fig. 5c) which yields proof for a constant intermolecular coupling of the $F_{40}PcCu$ molecules within the film and, hence, for a homogeneous structure of the film. Such an observation has also been reported earlier for $F_{64}PcCu$.[16] However, the spectra of solid $F_{64}PcCu$ matched well the solution spectrum indicating a very weak interaction of the molecules in the solid state caused by the strong suppression of electronic coupling by the bulky perfluoroisopropyl side groups.[16] Thus, the lower degree of fluorination in $F_{40}PcCu$ provides a strength of intermolecular coupling in solid state that is stronger than that for $F_{64}PcCu$, but weaker than that for $F_{16}PcCu$.[16,34]

3.3 Rate of the electron and ion transport in the $F_{40}PcCu$ films

In order to analyze the electron and ion transport within the $F_{40}PcCu$ films, cyclic voltammetry (CV) was performed at different scan rates ν. The initial cycle of the as-deposited films showed subtle differences in shape compared to subsequent cycles. Such conditioning, already reported for other fluorinated phthalocyanine films[17,18] was assigned to an initial hindrance of counter ion intercalation into the van der Waals-bonded molecular crystals. However, after about 6 cycles, reproducible CV curves could be obtained for all the prepared $F_{40}PcCu$ films (Fig. 6a), a change which can be assigned to the reversible reduction and re-oxidation of the $F_{40}PcCu$ films with concurrent intercalation and expulsion of K^+ ions. In Fig. 6b and c the current density j was divided by the scan rate to compare the CV curves for different scan rates in one plot. One main peak of reduction and one peak of re-oxidation were observed. The smaller reduction peak at less negative potentials (around −0.4 V) was mainly observed for lower scan rates and thinner films and is most likely indicative of a small concentration of molecules in a slightly different environment. With increasing scan rate, the peak potential of the main reduction process E_{red} shifted slightly towards more negative potentials, while the peak potential E_{reox} of the re-oxidation process underwent a larger shift towards less negative values, typical for kinetically hindered reactions. When the positions of the main reduction peak of around $-1.04\ V \leq E_{red}(F_{40}PcCu) \leq -0.91\ V$ and the re-oxidation peak of around $-0.78\ V \leq E_{reox}(F_{40}PcCu) \leq -0.30\ V$ measured for the stabilized CV curves of the $F_{40}PcCu$ films (10 to 50 nm average film thickness) are compared to other fluorinated Pc, some differences are observed. Thus, the reduction of $F_{40}PcCu$ requires a higher driving force than that of $F_{16}PcCu$ or $F_{64}PcCu$
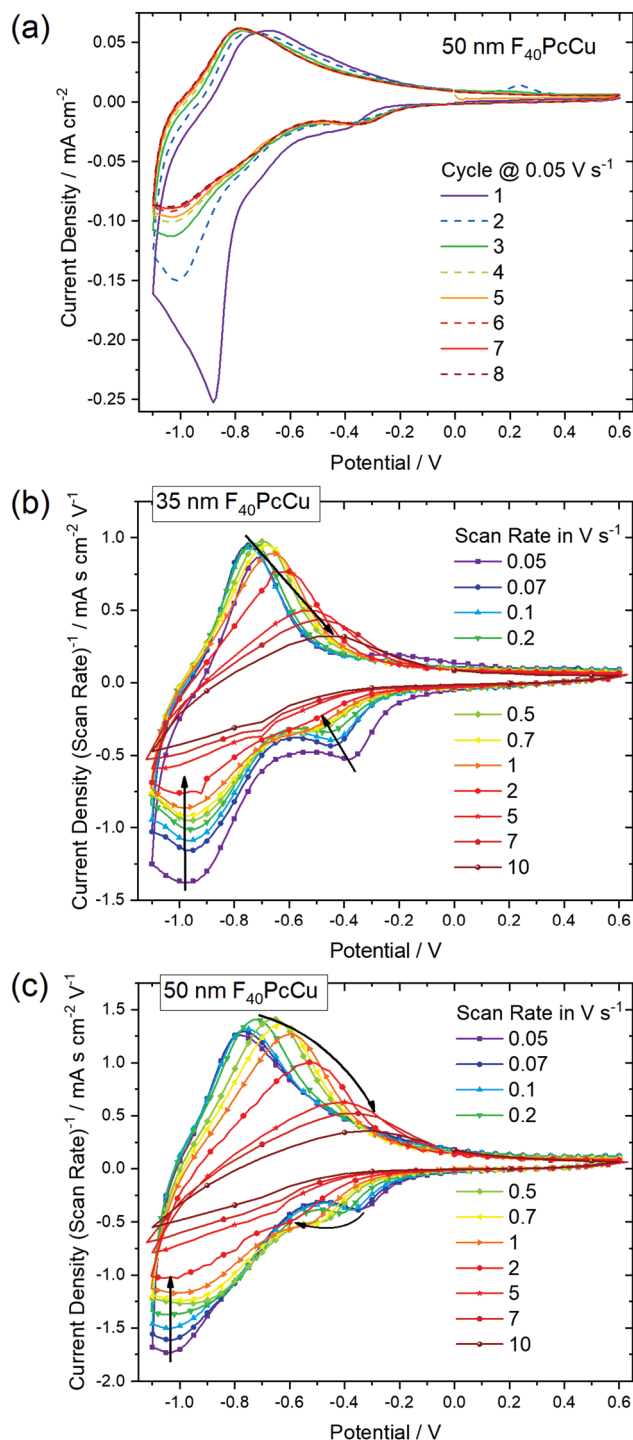
Fig. 6 Cyclic voltammograms of $F_{40}PcCu$ films in contact with 1 M aqueous KCl (a) with a film thickness of 50 nm during conditioning at a scan rate of 0.05 V s^{-1} and at different scan rates after conditioning of (b) a 35 nm and (c) a 50 nm thin film. In (b) and (c) the current density is divided by the scan rate to represent the CV curves in one plot.

-0.62 V $\leq E_{reox}(F_{64}PcCu) \leq -0.55$ V.[18] From the average value of $E_{red}(F_{40}PcCu)$ and $E_{reox}(F_{40}PcCu)$ the redox potential -0.91 V $\leq E(F_{40}PcCu) \leq -0.74$ V was estimated depending on the scan rate and thickness of the films. The values are more negative compared to the redox potential for $F_{16}PcCu$ or $F_{64}PcCu$ with -0.78 V $\leq E(F_{16}PcCu) \leq -0.64$ V[18] and $E(F_{64}PcCu) \approx -0.68$ V,[18] respectively suggesting that a slightly higher driving force is needed for reducing $F_{40}PcCu$ in solid state. This trend was found clearly more pronounced than in solution, speaking in favor of a higher intermolecular interaction energy in the neutral film of $F_{40}PcCu$ relative to the reduced film with inter-calated K$^+$ when compared to films of $F_{64}PcCu$ or $F_{16}PcCu$. From the values of the main reduction and the re-oxidation peak of the films up to a scan rate of 2 V s^{-1} an average peak potential difference of $\Delta E_p(F_{40}PcCu) = 0.30$ V was obtained, in the range of the values reported for films of $F_{16}PcCu$ and $F_{64}PcCu$ indicating (quasi-) reversibility of the redox processes[35,36] within all studied perfluorinated Pc films.[18]

To gain a deeper insight into the dependence of j on ν and, hence, the transport limitation within the films, the logarithm of the peak current densities of the cathodic (j_{pc}) as well as those of the anodic branches (j_{pa}) were plotted against the logarithm of the scan rates for different average film thicknesses (Fig. 7). A linear dependence of j on ν (slope of 1, solid black line) is assigned to films with reversible redox reactions without diffusion limitation, expected for an ideal adsorbed monolayer.[35] For reactions which are limited by the diffusion rate of counter ions, a dependence of j on the square root of ν is expected (slope of 0.5, dashed black line).[35] A slope of 0.6 (dotted black line) can be typically assigned to films where the reaction is limited by electron hopping between the redox centers.[37–39] Despite a decreasing j/ν for higher ν in the CV of Fig. 6,
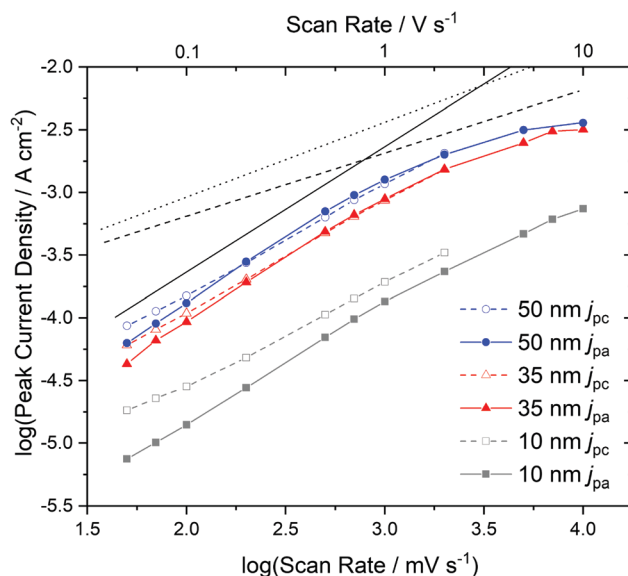

Fig. 7 Dependence of the cathodic (j_{pc}) and anodic (j_{pa}) peak current densities on the scan rate, determined by cyclic voltammetry with $F_{40}PcCu$ films of different thickness. The black dashed line indicates a slope of 0.5, the dotted line a slope of 0.6 and the solid line a slope of 1.

with -0.92 V $\leq E_{red}(F_{16}PcCu) \leq -0.76$ V and -0.79 V $\leq E_{red}(F_{64}PcCu) \leq -0.75$ V.[18] The values of E_{reox} for the re-oxidation process of $F_{40}PcCu$, however, were comparable with the reported values for $F_{16}PcCu$ with -0.71 V $\leq E_{reox}(F_{16}PcCu) \leq -0.38$ V, but in a slightly larger range compared to $F_{64}PcCu$ with

a linear dependence of the peak current on scan rates up to 1 V s^{-1} can still be fitted for the thicker films ($d \geq 35$ nm) in the reduction reaction and for all films in the re-oxidation reaction. Hence, the reduction of the films takes place with just a minor limitation by the transfer of electrons or counter ions and the re-oxidation reveals independence of any transport limitation, representing a high reversibility of the redox reactions of the films in this range of ν significantly larger than was observed for **F$_{16}$PcCu** and **F$_{64}$PcCu** films where a linear dependence could be observed only for $\nu < 0.2$ V s^{-1}.[18] For **F$_{16}$PcCu** this was only valid for $d \leq 20$ nm and for **F$_{64}$PcCu** for $d \leq 50$ nm.[18] For $\nu > 0.2$ V s^{-1} the **F$_{64}$PcCu** films thinner than 50 nm showed a dependence of $j \sim \nu^{0.6}$ characteristic for a limitation by electron hopping in the films and sufficiently fast diffusion of the counter ions through the **F$_{64}$PcCu** films, facilitated by the presence of the large perfluoroisopropyl substituents.[18] At scan rates $\nu > 1$ V s^{-1} the linear dependence of j on ν is no longer observed, but the reaction clearly becomes transport-limited. A clear assignment to a characteristic slope is no longer possible because for **F$_{40}$PcCu** films with $d \geq 35$ nm a dependence of $j \sim \nu^{0.5}$ was indicated, whereas the 10 nm **F$_{40}$PcCu** film approached $j \sim \nu^{0.6}$. Therefore, limitation by either the counter ions (slope of 0.5) or by hopping of electrons (slope of 0.6) cannot be distinguished, the transport of both seems to be equally fast. It should be noted that **F$_{40}$PcCu** films show no transport limitation up to a scan rate 5 times higher than that reported for **F$_{16}$PcCu** and **F$_{64}$PcCu**.[18] Thus, the two isoindole units with two perfluoroisopropyl substituents in **F$_{40}$PcCu** instead of four such units in **F$_{64}$PcCu**[16] (Fig. 1) lead to a film structure with optimized attributes of both **F$_{16}$PcCu** and **F$_{64}$PcCu** which allows a fast electron as well as a fast ion transport through the film.

As a quantitative measure for the rate of transport in the **F$_{40}$PcCu** films, an effective diffusion coefficient D was obtained from chronoamperometric measurements. After the initialization of the film during the first cycle, the subsequent cycles were invariable. The integrated current density yielded an average charge of 1.5 electrons for each deposited molecule of **F$_{40}$PcCu** considering the molecular weight of 1464.01 g mol^{-1}. The measured cathodic and anodic current densities of the second cycle were plotted against the reciprocal square root of time $t^{-1/2}$ (Fig. 8) corresponding to the Cottrell eqn (1) valid for semi-infinite diffusion

$$j = nFcD^{1/2}\pi^{-1/2}t^{-1/2} \qquad (1)$$

where F is Faraday's constant, n is the number of electrons transferred in the reaction and c is the concentration in the bulk of the electrolyte.[35] The characteristics, Fig. 8, are reminiscent of those reported for films of redox polymers like poly(fluorenone-bithiophene)[40] or for redox polyelectrolyte multilayers.[41] In the long time regime the current density decreased to lower than expected values, an observation which can be explained by the finite film thickness leading to deviations from semi-infinite diffusion. In the short time regime of 4.4–10 ms (10–15 s$^{-1/2}$) the data followed the expected linear Cottrellian behavior and allow a quantitative analysis.

For the 35 nm thin film, values for the effective diffusion coefficient of $D_c(35 \text{ nm}) = 4.4 \times 10^{-10}$ cm^2 s^{-1} and $D_a(35 \text{ nm}) = 1.4 \times 10^{-9}$ cm^2 s^{-1} were obtained from the fits of the cathodic and anodic current densities, respectively, Fig. 8a. The values estimated for a 50 nm thin film are in the same range, with $D_c(50 \text{ nm}) = 5.3 \times 10^{-10}$ cm^2 s^{-1} and $D_a(50 \text{ nm}) = 1.9 \times 10^{-9}$ cm^2 s^{-1}. For both films, the values of D_a for the re-oxidation were found higher than those of D_c for the reduction, as found earlier for **F$_{16}$PcCu**.[18] Such smaller effective diffusion coefficient upon reduction might be caused by a slow removal of the solvation shell[42] before intercalation into the solid film of **F$_{40}$PcCu**.

The values of the diffusion coefficient reported for **F$_{16}$PcCu**, $D_c(\textbf{F}_{16}\textbf{PcCu}) = 8 \times 10^{-11}$ cm^2 s^{-1} and $D_a(\textbf{F}_{16}\textbf{PcCu}) = 1.5 \times 10^{-10}$ cm^2 s^{-1}, as well as $D_c(\textbf{F}_{64}\textbf{PcCu}) = D_a(\textbf{F}_{64}\textbf{PcCu}) = 5 \times 10^{-11}$ cm^2 s^{-1} for **F$_{64}$PcCu** were significantly smaller[18] compared to the values for **F$_{40}$PcCu**. Thus, the faster diffusion in **F$_{40}$PcCu** is a direct confirmation for the successfully enhanced overall
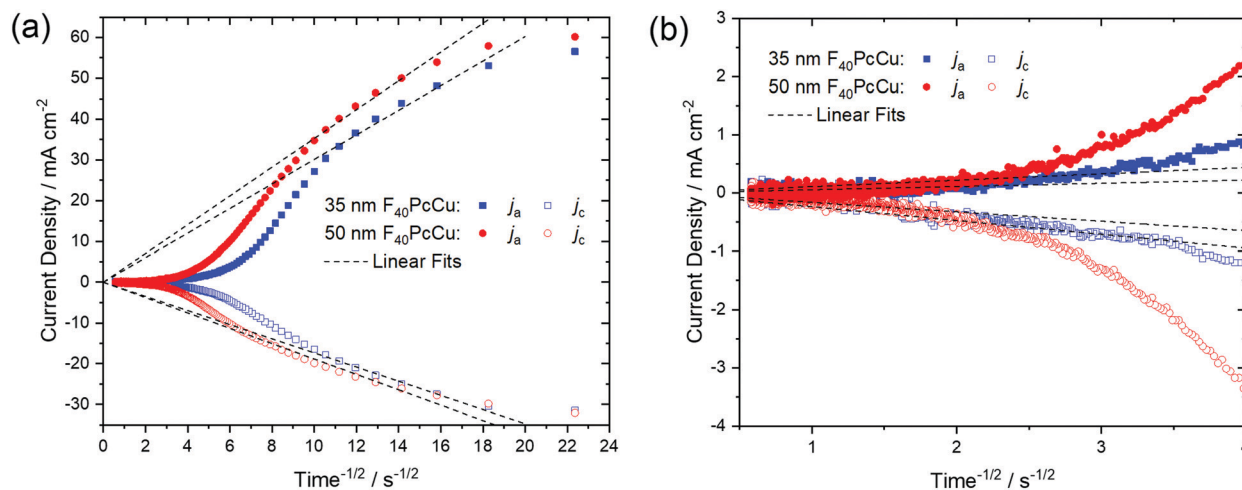

Fig. 8 (a) Cathodic (j_c) and anodic (j_a) current densities dependent on the reciprocal square root of time obtained from chronoamperometric analysis of a 35 nm (blue) and 50 nm (red) thin **F$_{40}$PcCu** film. (b) Plot of the data for long times. The linear fits according to the Cottrell equation are marked in dashed lines.

diffusion of electrons and K$^+$ within the film. By zooming into the range of the data at longer times around 4 s$^{-1/2}$, as shown in Fig. 8b, another linear region was observed. The fits in this time regime yielded considerably smaller diffusion coefficients of $D = 0.5$–8.5×10^{-12} cm^2 s^{-1}, representing a lower limit for the diffusion into those parts of films which are least accessible, either because of poor electronic conduction or difficult intercalation of ions. However, for the overall yield of the reaction and, hence, prospective technical application of the reactions, the high values of D in the early stage of the reactions are most significant since they represent the highest currents and, hence, the largest contribution. Along with the results from the CV measurements (Fig. 7) revealing a transport limitation in the films dominated by neither electrons nor ions, but given by a similarly fast movement of both with $j \sim \nu$ up to 1 V s^{-1}, it can be concluded that the moderate intermolecular coupling of the **F$_{40}$PcCu** molecules provides facilitated pathways for both ions and electrons in the films.

3.4 Spectroelectrochemical characterization of F$_{40}$PcCu films

Optical absorption spectra of the **F$_{40}$PcCu** films were measured *in situ* during the electrochemical measurements to (i) investigate the changes of the electronic structure of the molecules in the solid state caused by the redox processes and (ii) to analyze the performance of these films as possible electrochromic smart windows.

The changes in the electronic structure of the **F$_{40}$PcCu** films observed in the stabilized CV curves are clearly reflected in the absorption spectra of the films, as shown in Fig. 9. As expected, the bands of the neutral films upon immersion into the aqueous KCl solution were found almost equal to those of the as-deposited films (Fig. 5). However, a small but significant shift of the Q-band maximum to about 630 nm was caused by this different environment. In contrast to earlier experiments with **F$_{16}$PcCu**,[18] the electrochemical conditioning of **F$_{40}$PcCu** did not lead to any changes in the spectra, *i.e.* the intermolecular

coupling was found unchanged following the first eight cycles of reduction and re-oxidation.

The reduction of **F$_{40}$PcCu** led to remarkable changes in the Q-band position as well as in the absorptions between the Soret and the Q-band, while the absorption of the Soret band was just slightly decreased without any remarkable shift. The absorption maximum at 630 nm decreased in intensity while the shoulder at around 690 nm transformed into a local maximum. A new absorption maximum at around 540 nm and a broad absorption in the NIR at 800 nm and beyond, both typical for phthalocyanine rings in their reduced state (Pc(-3)Cu(II)) arose (Fig. 9a) as also observed for **F$_{16}$PcCu**[18] and for **F$_{64}$PcCu**.[17,18] Upon re-oxidation these spectral changes were reversed (Fig. 9b). Well-defined isosbestic points were detected at 390 nm, characteristic of a uniformly smaller absorption by the Soret band in the reduced state. Small ranges of intersecting spectra ("isosbestic ranges") were detected around 580 nm and around 730 nm upon re-oxidation of the films, indicating widely uniform transitions also in the Q-band range, which is known to be very sensitive to parameters of intermolecular coupling in Pc.[28] These ranges were considerably wider upon reduction of the film, consistent with the two contributions in the cathodic wave of the CV (Fig. 6). The presence of isosbestic points and "isosbestic ranges" indicates the reversible $A \leftrightarrow B$ transformation of neutral species A to a reduced species B with characteristic spectra for neutral (re-oxidized) A and reduced B species, similar to results for **F$_{64}$PcCu** films reported earlier[17,18] confirming the presence of a reversible redox reaction, with no permanent change in the material.

In order to check if a complete reduction and re-oxidation of the films was ensured even for faster scan rates, which would be beneficial for fast switching in electrochromic layers, the change in optical absorption between the reduced (-1.1 V) and the re-oxidized state (0.6 V) of the films was determined in dependence of the scan rate (Fig. 10). Absorption signals at 540 nm and 630 nm, for which most significant changes were detected upon reduction and re-oxidation were selected (marked with arrows in Fig. 9).
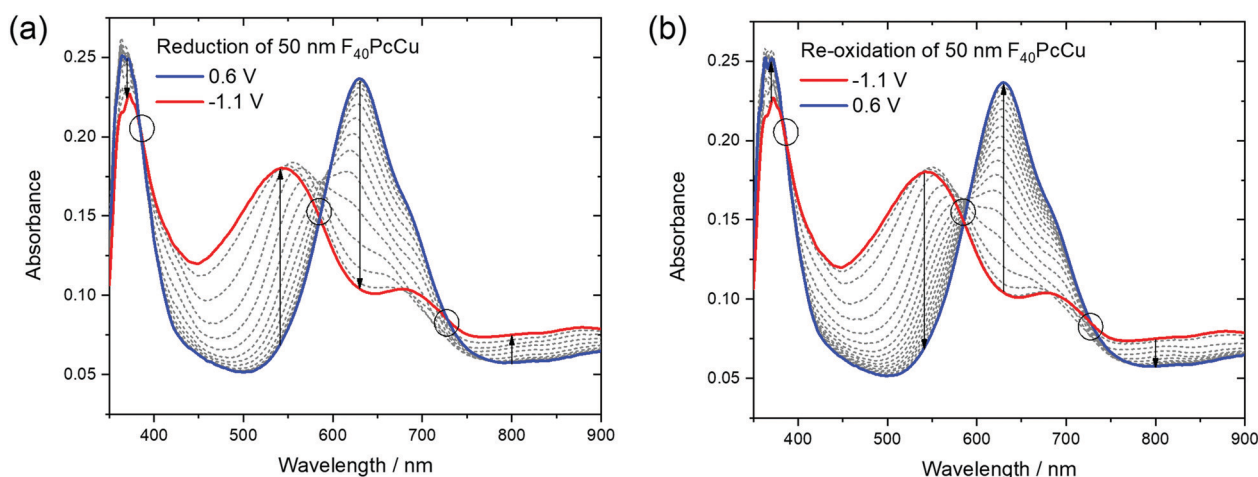

Fig. 9 Optical absorption spectra of a 50 nm thin film of **F$_{40}$PcCu** measured during cyclic voltammetry at 0.05 V s^{-1} upon (a) reduction and (b) re-oxidation of the film. The isosbestic points and ranges are marked by circles.

7706 | *Phys. Chem. Chem. Phys.*, 2020, **22**, 7699–7709

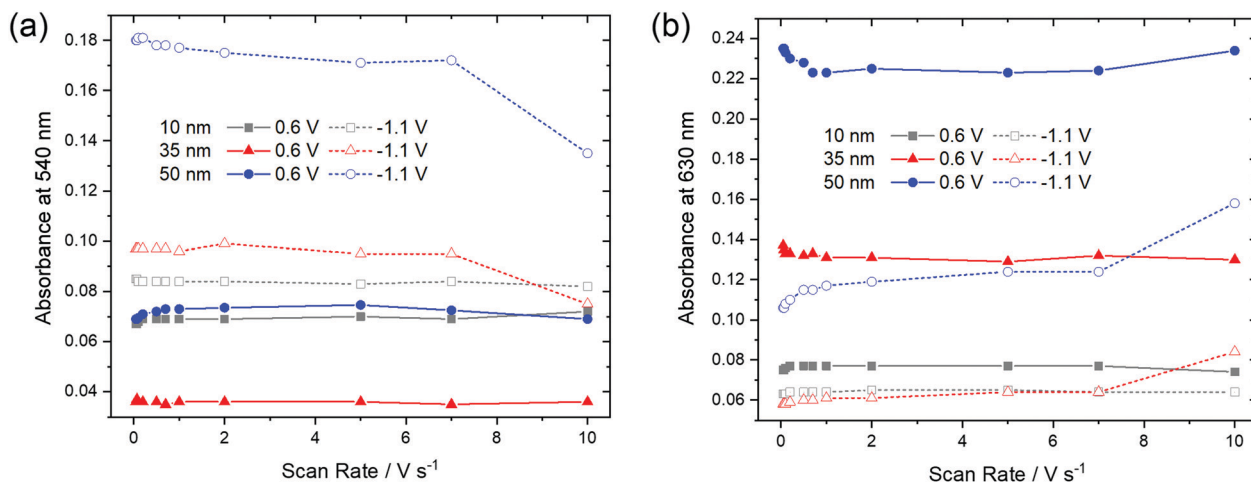This journal is © the Owner Societies 2020

Fig. 10 Optical absorbance at (a) 540 nm and (b) 630 nm as a function of scan rate of $F_{40}PcCu$ films of different thickness in the re-oxidized (0.6 V) or reduced (−1.1 V) states.

For the thinnest, 10 nm film of $F_{40}PcCu$ the absorbances at 540 nm and 630 nm remained largely constant for all scan rates. The main observation, however, is that the thicker films showed significant changes at higher scan rates. Upon reduction (−1.1 V), the absorbance at 540 nm has a lower value, indicating incomplete reduction of the film. Correspondingly, a higher
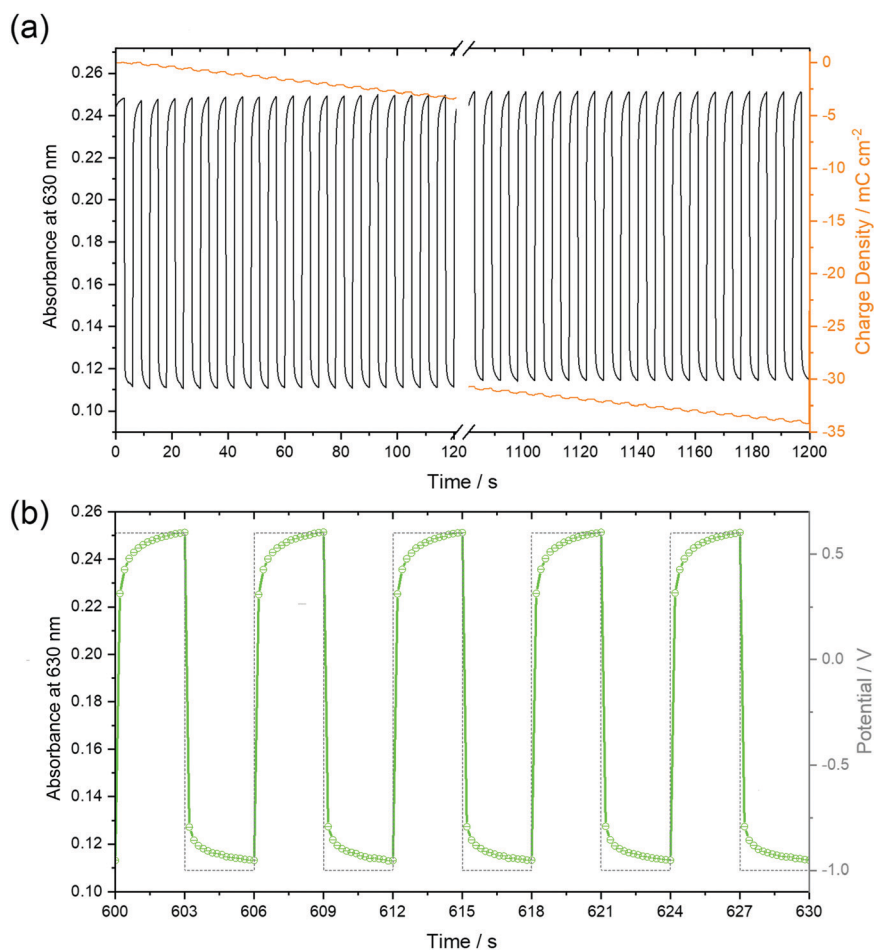

Fig. 11 Optical absorption at 630 nm of a 50 nm thin $F_{40}PcCu$ film, recorded during chronoamperometry over 20 minutes (a) and at high resolution for an intermediate time interval (b) between the potentials depicted as dashed profiles in (b). The variation of the charge density within 200 cycles is shown as orange lines in (a).

absorbance was found at 630 nm, characteristic of remaining neutral molecules. These features are most significant for the 50 nm thin film for which changes were noticeable at scan rates $\nu > 1 \text{ V s}^{-1}$. Both trends clearly point at an incomplete reduction of the films at high scan rates. Upon re-oxidation (0.6 V), however, absorbance remained almost constant even for higher scan rates and thicker films, confirming the fast re-oxidation processes, also indicated by the higher effective diffusion coefficient determined during re-oxidation (Fig. 8).

3.5 Long-term, repeated switching characteristics of $\mathbf{F_{40}PcCu}$ films

The stability of the time-dependent switching characteristics was studied by chronoamperometry of 50 nm thin films over 20 minutes (Fig. 11). It is remarkable that the absorbance, as shown in Fig. 11a for the 50 nm thin film in both the reduced and neutral states remained constant for all subsequent 200 cycles, thus defining a reversible switching process which, in turn, indicated a high stability of the films. Despite this stability, the total charge monotonously shifted to negative values indicative of a background current at the negative potential as already observed by CV (Fig. 6), in earlier studies at $\mathbf{F_{16}PcCu}$ and $\mathbf{F_{64}PcCu}$ films, and assigned to water reduction.[17,18] Obviously, this side reaction had no influence on the spectral properties of the film, a feature also found for $\mathbf{F_{16}PcCu}$ and $\mathbf{F_{64}PcCu}$ films using Li^+ or K^+ as counter ions.[17,18] The higher time resolution (Fig. 11b) indicates fast decrease of the absorbance at 630 nm upon reduction (-1.0 V) and recovery upon re-oxidation (0.6 V). The response times, $0.2 \text{ s} \leq t_{\text{red}} \leq 0.4 \text{ s}$ and $0.3 \text{ s} \leq t_{\text{reox}} \leq 0.4 \text{ s}$ were determined, corresponding to the time needed to switch the absorption to 90% of the change to the reduced or the neutral state, respectively. The present response times (Fig. 11) are shorter than the 1.3 s and 0.6 s values, determined in earlier work for the reduction and re-oxidation of $\mathbf{F_{64}PcCu}$ films,[17] revealing a faster switching behavior of the present films caused by facilitated transport of both electrons and K^+ counter ions in $\mathbf{F_{40}PcCu}$ as directly seen in cyclic voltammetry (Fig. 7) and the chronoamperometric measurements (Fig. 8). The films provide fast and reversible switching capabilities, stable over many cycles, ideal for their use as electrochromic materials.

4 Conclusions

A new type of perfluorinated phthalocyanine, namely $\mathbf{F_{40}PcCu}$ has been designed to exhibit simultaneously both efficient electron and ion transport properties. The molecule in solution shows the expected absorption bands of phthalocyanines and exhibits facile reduction and re-oxidation. Thin films, obtained by physical vapor deposition exhibited spectral broadening of the absorption spectra characteristic for thin films of weakly coupling chromophores in solid state. Electrochromic cells could be obtained by a contact of each individual grain of the films with the FTO support and the aqueous electrolyte. The reversible switching observed upon reduction and re-oxidation

indicates a high stability of the films with no permanent change in the material. Changes of the absorption spectra in the reduced state typical for phthalocyanines ($Pc(-3)Cu(II)$) were noticed. The electrochemical characteristics of thin films showed that $\mathbf{F_{40}PcCu}$ films exhibited intermolecular coupling within the grains, weaker than that for $\mathbf{F_{16}PcCu}$, but stronger than that for $\mathbf{F_{64}PcCu}$, leading to a facilitated transport of both electrons and counter ions up to scan rates of about 1 V s^{-1}. Short response times during the switching process were determined for both the reduction and re-oxidation of the films. However, at very high scan rates the films could not be fully reduced, whereas a fast re-oxidation of the films was still observed. The apparent diffusion coefficient ranges from 10^{-10} to 10^{-9} cm^2 s^{-1} depending on film thicknesses, a characteristic of fast reversible switching attractive for the use of the new material in electrochromic smart windows.

Conflicts of interest

There are no conflicts of interest to declare.

Acknowledgements

References

1 H. Klauk, *Organic Electronics*, Wiley-VCH, Weinheim, 2006.
2 C. G. Granqvist, *Thin Solid Films*, 2014, **564**, 1–38.
3 R. Baetens, B. P. Jelle and A. Gustavsen, *Sol. Energy Mater. Sol. Cells*, 2010, **94**, 87–105.
4 P. R. Somani and S. Radhakrishnan, *Mater. Chem. Phys.*, 2002, **77**, 117–133.
5 R. J. Mortimer, A. L. Dyer and J. R. Reynolds, *Displays*, 2006, **27**, 2–18.
6 M. Berggren, X. Crispin, S. Fabiano, M. P. Jonsson, D. T. Simon, E. Stavrinidou, K. Tybrandt and I. Zozoulenko, *Adv. Mater.*, 2019, **31**, e1805813.
7 A. L. Dyer, A. M. Österholm, D. E. Shen, K. E. Johnson and J. R. Reynolds, in *Electrochromic Materials and Devices*, ed. R. J. Mortimer, D. R. Rosseinsky and P. M. S. Monk, Wiley-VCH, Weinheim, 2015, ch. 5, vol. 1, pp. 113–184.
8 L. Beverina, G. A. Pagani and M. Sassi, *Chem. Commun.*, 2014, **50**, 5413–5430.
9 M. M. Nicholson, in *Phthalocyanines: Properties and Applications*, ed. C. C. Leznoff and A. B. P. Lever, VCH, Weinheim, 1993, ch. 2, vol. 3, pp. 71–118.

7708 | *Phys. Chem. Chem. Phys.*, 2020, **22**, 7699–7709

This journal is © the Owner Societies 2020

10 J. M. Green and L. R. Faulkner, *J. Am. Chem. Soc.*, 1983, **105**, 2950–2955.

11 B. Schumann, D. Wöhrle and N. I. Jaeger, *J. Electrochem. Soc.*, 1985, **132**, 2144–2149.

12 C. Wang, H. Dong, L. Jiang and W. Hu, *Chem. Soc. Rev.*, 2018, **47**, 422–500.

13 M. K. Engel, in *The Porphyrin Handbook*, ed. K. M. Kadish, K. M. Smith and R. Guilard, Academic Press, San Diego, 2003, vol. 20, pp. 1–242.

14 T. Hosokai, A. Gerlach, A. Hinderhofer, C. Frank, G. Ligorio, U. Heinemeyer, A. Vorobiev and F. Schreiber, *Appl. Phys. Lett.*, 2010, **97**, 63301.

15 L. Cornelius, M. Beu, C. Keil and D. Schlettwein, *Phys. Status Solidi RRL*, 2012, **6**, 214–216.

16 C. Keil, O. Tsaryova, L. Lapok, C. Himcinschi, D. Wöhrle, O. R. Hild, D. R. T. Zahn, S. M. Gorun and D. Schlettwein, *Thin Solid Films*, 2009, **517**, 4379–4384.

17 S. Nagel, M. Lener, C. Keil, R. Gerdes, Ł. Łapok, S. M. Gorun and D. Schlettwein, *J. Phys. Chem. C*, 2011, **115**, 8759–8767.

18 J. Weissbecker, A. Loas, S. M. Gorun and D. Schlettwein, *Electrochim. Acta*, 2015, **157**, 232–244.

19 S. M. Gorun, B. A. Bench, G. Carpenter, M. W. Beggs, J. T. Mague and H. E. Ensley, *J. Fluorine Chem.*, 1998, **91**, 37–40.

20 A. B. P. Lever, E. R. Milaeva and G. Speier, in *Phthalocyanines: Properties and Applications*, ed. C. C. Leznoff and A. B. P. Lever, VCH, Weinheim, 1993, vol. 3, ch. 1.

21 H. H. Patel, PhD thesis, Seton Hall University, 2015.

22 E. N. Carrión, A. Loas, H. H. Patel, M. Pelmuș, K. Ramji and S. M. Gorun, *J. Porphyrins phthalocyanines*, 2018, **22**, 371–397.

23 K. J. M. Nolan, M. Hu and C. C. Leznoff, *Synlett*, 1997, 593–594.

24 H. Konami, Y. Ikeda, M. Hatano and K. Mochizuki, *Mol. Phys.*, 1993, **80**, 153–160.

25 H. Moons, Ł. Łapok, A. Loas, S. van Doorslaer and S. M. Gorun, *Inorg. Chem.*, 2010, **49**, 8779–8789.

26 K. Hesse and D. Schlettwein, *J. Electroanal. Chem.*, 1999, **476**, 148–158.

27 D. Schlettwein, N. I. Jaeger and T. Oekermann, in *The Porphyrin Handbook*, ed. K. M. Kadish, K. M. Smith and R. Guilard, Academic Press, San Diego, 2003, vol. 16, pp. 247–284.

28 C. G. Claessens, U. Hahn and T. Torres, *Chem. Rec.*, 2008, **8**, 75–97.

29 A. W. Snow, in *The Porphyrin Handbook*, ed. K. M. Kadish, K. M. Smith and R. Guilard, Academic Press, San Diego, 2003, vol. 17, pp. 129–176.

30 C. Keil, PhD thesis, Justus-Liebig-University, 2012.

31 D. G. de Oteyza, E. Barrena, J. O. Ossó, S. Sellner and H. Dosch, *J. Am. Chem. Soc.*, 2006, **128**, 15052–15053.

32 R. Ye, M. Baba, Y. Ohishi, K. Mori and K. Suzuki, *Mol. Cryst. Liq. Cryst.*, 2006, **444**, 203–210.

33 G. Liu, T. Gredig and I. K. Schuller, *Europhys. Lett.*, 2008, **83**, 56001.

34 W. Michaelis, D. Wöhrle and D. Schlettwein, *J. Mater. Res.*, 2004, **19**, 2040–2048.

35 A. J. Bard and L. R. Faulkner, *Electrochemical Methods*, Wiley, New York, 2001.

36 J.-M. Savéant, *Elements of Molecular and Biomolecular Electrochemistry*, John Wiley & Sons, Hoboken, NJ, 2006.

37 E. Laviron, *J. Electroanal. Chem.*, 1980, **112**, 1–9.

38 E. Laviron, L. Roullier and C. Degrand, *J. Electroanal. Chem.*, 1980, **112**, 11–23.

39 E. Laviron, *J. Electroanal. Chem.*, 1981, **122**, 37–44.

40 M. D. Levi, R. Demadrille, A. Pron, M. A. Vorotyntsev, Y. Gofer and D. Aurbach, *J. Electrochem. Soc.*, 2005, **152**, E61–E67.

41 M. Tagliazucchi, D. Grumelli, C. Bonazzola and E. J. Calvo, *J. Nanosci. Nanotechnol.*, 2006, **6**, 1731–1740.

42 K. Xu, A. von Cresce and U. Lee, *Langmuir*, 2010, **26**, 11538–11543.

This journal is © the Owner Societies 2020

Phys. Chem. Chem. Phys., 2020, **22**, 7699–7709 | **7709**